

Direct identification of predator-prey dynamics in gyrokinetic simulations

Sumire Kobayashi, Özgür D Gürçan, and Patrick H. Diamond

Citation: *Physics of Plasmas* **22**, 090702 (2015); doi: 10.1063/1.4930127

View online: <http://dx.doi.org/10.1063/1.4930127>

View Table of Contents: <http://scitation.aip.org/content/aip/journal/pop/22/9?ver=pdfcov>

Published by the AIP Publishing

Articles you may be interested in

[Gyrokinetic turbulence cascade via predator-prey interactions between different scales](#)

Phys. Plasmas **22**, 050702 (2015); 10.1063/1.4920965

[A plasma source driven predator-prey like mechanism as a potential cause of spiraling intermittencies in linear plasma devices](#)

Phys. Plasmas **21**, 032302 (2014); 10.1063/1.4867492

[Robustness of predator-prey models for confinement regime transitions in fusion plasmas](#)

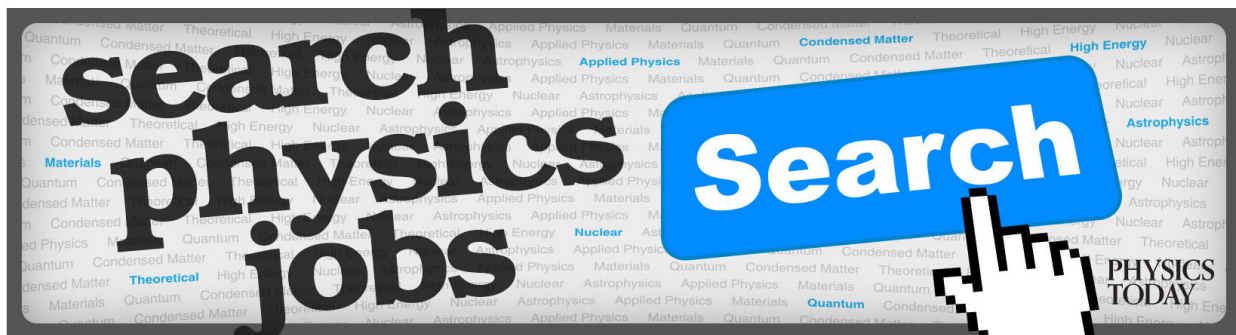
Phys. Plasmas **20**, 042302 (2013); 10.1063/1.4800009

[Gyro-kinetic simulation of global turbulent transport properties in tokamak experiments](#)

Phys. Plasmas **13**, 092505 (2006); 10.1063/1.2338775

[Gyrokinetic simulations of ion and impurity transport](#)

Phys. Plasmas **12**, 022305 (2005); 10.1063/1.1848544



Direct identification of predator-prey dynamics in gyrokinetic simulations

Sumire Kobayashi,^{1,a)} Özgür D Gürçan,¹ and Patrick H. Diamond²

¹Laboratoire de Physique des Plasmas, CNRS, Paris-Sud, Ecole Polytechnique, UMR7648, F-91128 Palaiseau, France

²University of California, San Diego, La Jolla, California 92093-0319, USA

(Received 12 June 2015; accepted 17 August 2015; published online 10 September 2015)

The interaction between spontaneously formed zonal flows and small-scale turbulence in nonlinear gyrokinetic simulations is explored in a shearless closed field line geometry. It is found that when clear limit cycle oscillations prevail, the observed turbulent dynamics can be quantitatively captured by a simple Lotka-Volterra type predator-prey model. Fitting the time traces of full gyrokinetic simulations by such a reduced model allows extraction of the model coefficients. Scanning physical plasma parameters, such as collisionality and density gradient, it was observed that the *effective* growth rates of turbulence (i.e., the prey) remain roughly constant, in spite of the higher and varying level of primary mode linear growth rates. The effective growth rate that was extracted corresponds roughly to the zonal-flow-modified primary mode growth rate. It was also observed that the effective damping of zonal flows (i.e., the predator) in the parameter range, where clear predator-prey dynamics is observed, (i.e., near marginal stability) agrees with the collisional damping expected in these simulations. This implies that the Kelvin-Helmholtz-like instability may be negligible in this range. The results imply that when the tertiary instability plays a role, the dynamics becomes more complex than a simple Lotka-Volterra predator prey. © 2015 AIP Publishing LLC. [<http://dx.doi.org/10.1063/1.4930127>]

Turbulence is one of the important aspects of collective plasma behavior in magnetic confinement devices whose understanding requires further study in order to elucidate the limitations on confinement time. In particular, the self regulation of plasma turbulence by zonal flows is a key issue with important potential for the reduction of turbulent transport. Limit cycle oscillations, closely resembling predator-prey dynamics between fluctuations and large scale plasma flows (i.e., radial electric fields), have been observed in various confinement devices during the transition from the low (L) to high (H) confinement. The limit cycle oscillations between zonal flows and fluctuations cause the pressure gradient to oscillate as a result of quenching of the turbulent transport, this allows the system to explore different values of the pressure gradient and thus go from one fixed point corresponding to the L-mode to the other one, corresponding to the H-mode.

Previous works demonstrated that gyrokinetic simulations of closed field line Z-pinch system display distinct predator-prey dynamics between the zonal and the fluctuating non-zonal components of the electrostatic potential (i.e., ϕ_q and ϕ_k , respectively, where ϕ is normalized to $T_0\rho_0 eR$), with the particle and heat flux naturally following the non-zonal component.¹ It was also found that the primary mode growth rates of gyrokinetic simulations become suppressed in the presence of zonal flows.¹ These results were in accordance with what was already known about the dynamics and behavior of plasma turbulence and zonal flows in tokamaks.² In particular, the similarity of these results to ion temperature

gradient (ITG) turbulence in sheared magnetic field³ indicates the robustness of the predator-prey paradigm in diverse modes and geometries.

In the context of magnetic fusion plasmas, self-regulation of the micro-turbulence by zonal flows, and the resulting predator-prey oscillations are thought to be important for the Low to High confinement (L-H) transition.⁴⁻⁷ Limit cycle oscillations that may be linked to this dynamics have been observed in a number of confinement devices during the L-H transition.⁸⁻¹² Similar dynamics (with a dominant zonal flow acting as the top predator) also play an important role in the wave-number cascade by self-generated zonal flows.¹³⁻¹⁶

Here, we explore the interactions between spontaneously formed zonal flows and small-scale turbulence caused by linear instabilities with five-dimensional nonlinear gyrokinetic GS2 flux-tube simulations^{17,18} of the Z-pinch geometry, in which a cylindrically symmetric plasma is confined by a poloidal magnetic field $B_\theta(r)$ and compare the results with a simple predator-prey model. In Fig. 1, the predator-prey behavior is shown between the non-zonal and zonal energies: $N = \sum_k |\phi_k|^2 (1 + k^2)$ and $E_v = |\phi_q|^2 q^2$, where q is the zonal flow wavenumber.

Subsequently, the following Lotka Volterra equations are adopted, in order to fit the time traces of both the zonal and the fluctuation energy from gyrokinetic simulations with various values of collisionality ν (normalized to $\nu_{phys} = \nu\sqrt{2}v_{thi}/R$) and the density gradient L_n/R . The Lotka Volterra model can be written as

$$\frac{\partial N}{\partial t} = \gamma_{eff} N - c_1 N E_v, \quad (1)$$

^{a)}Electronic mail: sumire.kobayashi@lpp.polytechnique.fr

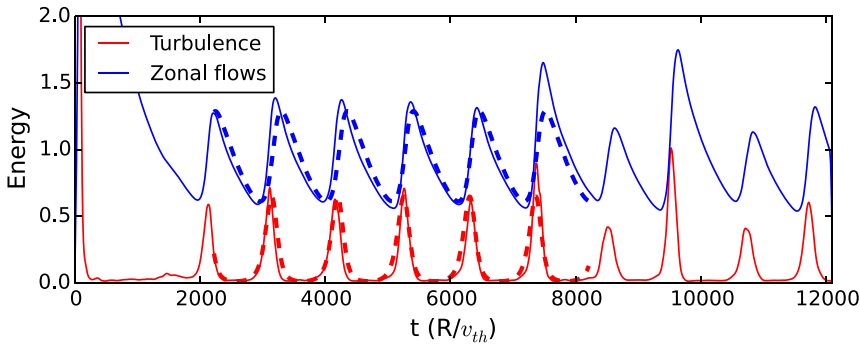


FIG. 1. Energy as a function of time, for zonal (blue) and non-zonal (red) components for $\nu=0.005$ and $R/L_n=1.4$ in a gyrokinetic simulation. The results can be fitted by simple predator-prey model (shown in dashed lines).

$$\frac{\partial E_v}{\partial t} = c_2 E_v N - \gamma_Z E_v, \quad (2)$$

where γ_{eff} is the effective linear growth rate of the prey, c_1 and c_2 (usually $c_1=c_2$ with a given normalization of N and E_v implying a conservation law between the zonal and the non-zonal components) are the nonlinear interaction coefficients between the predator and the prey, and γ_Z is the zonal flow damping rate. Additional terms such as a damping term proportional to $\Delta\omega N^2$ in (1), where $\Delta\omega$ is the nonlinear decorrelation rate, and a nonlinear damping term with $\gamma_{nl} E_v^2$ in (2) where γ_{nl} is a nonlinear zonal damping are common extensions to the standard Lotka Volterra model used in the plasma context.¹⁹ In this formulation, the prey has an internal growth proportional to γ_{eff} with a nonlinear shear decorrelation proportional to c_1 and a possible nonlinear damping (i.e., eddy damping) proportional to $\Delta\omega$, while the predator has a linear damping proportional to γ_Z but a nonlinear growth due to coupling to turbulence proportional to c_2 and a possible nonlinear damping proportional to γ_{nl} .

Predator-prey dynamics has been extensively studied in the context of coupled population dynamics in ecosystems of competing species. This simple idea has a wide range of applications across different disciplines from actual predator-prey²⁰ to host-parasite²¹ to immune system-tumor cell²² interactions as well as dynamics of substitution/innovation in the adoption of new technologies²³ and interaction of social agents.²⁴ As discussed earlier, turbulence and zonal flows in tokamak experiments during limit cycles are known to display the predator-prey-like behaviour as well.^{8,16} Nonetheless the detailed mechanism of these observed limit cycle oscillations in tokamaks have not been fully understood.

The gyrokinetic simulations are performed for a Z-pinch plasma with $\beta \ll 1$, where the fluctuations are electrostatic and two dimensional. It was shown in previous studies that this simple geometry produces results consistent with dipolar fusion and planetary magnetosphere experiments (LDX at MIT-Columbia University and RT-1 at University of Tokyo^{25,26}), and it shares some important characteristics with other magnetized confinement configurations including the tokamak.²⁷⁻²⁹ The system is stable to MHD instabilities when the gradients are sufficiently weak, in which case the dominant primary instability is the so-called entropy-mode.³⁰ This primary instability is in fact a plasma analogue of the Rayleigh-Bénard instability in ordinary fluids, where curvature effects, part of which is the centrifugal force, play

a role analogous to gravity in R-B convection, modified by finite Larmor radius effects. Considering an equilibrium with equal ion and electron temperatures $T_i=T_e$, $L_n/L_T=0$, where $L_n^{-1}=\frac{1}{n_0} \frac{dn}{dr}$ and $L_T^{-1}=\frac{1}{T_0} \frac{dT}{dr}$ are the inverse density and temperature gradient scale lengths, taking $k_\perp \rho_i \ll 1$, where k_\perp is the wavevector perpendicular to the background magnetic field B_0 , $\rho_i=v_{thi}/\omega_{ci}$ is the ion gyroradius, $\omega_{ci}=eB_0/m_i c$ is the ion gyrofrequency, $v_{thi}=\sqrt{T_i/m_i}$ is ion thermal velocity, m_i is ion mass, e is an electron charge, and c is the speed of light, and assuming that the collisions are sufficiently strong, the simple expression from two-fluid theory predicts an instability threshold such that $10/7 < R/L_n < 10/3$, where R is the radius of curvature. The gyrokinetic simulations with arbitrary collisionalities usually exhibit a threshold which is about 15% lower.^{1,29} The simulations are performed with realistic mass ratio (i.e., $m_i/m_e=1836$) and the model conserves total energy, momentum, and particle number.

As shown in the dashed lines in Fig. 1, the interaction dynamics observed in those gyrokinetic simulations can be captured reasonably well with the simple predator-prey equations. Each parameter of the model can be estimated by fitting it to the gyrokinetic simulations, treating the full solution of the Lotka-Volterra system (with the same initial condition as the considered window of gyrokinetic simulation data) as a “fitting function” and the model parameters as the fitting variables. Here, for the purpose of demonstration of the principle, we have used least squares fitting. However, we believe that the fitting technique can be improved in order to include cases where the predator-prey oscillations are less prominent, and the system starts to transition to chaotic behavior (i.e., period doubling, etc.). The field of extracting models from chaotic data (e.g., Ref. 31) is a vast field of research and certain features of the candidate models can be used in simplifying the task of fitting (e.g., Refs. 32 and 33). We leave these perspectives to future work.

Obtaining the model parameters by the fitting procedure allows us to compare the gyrokinetic collisionality ν and the zonal flow damping rate estimated by the model γ_{zf} (normalized to v_{thi}/R), with the assumption that $\gamma_Z \sim \gamma_{zf} q^2$, where q (normalized to $1/\rho_i$) is the wavenumber of the dominant zonal flow component (here $q=0.5$). Notice that since a 2D slab formulation is used, the zonal flow damping is expected to have the form of viscosity, whereas in a tokamak, due to toroidal geometry leading to friction between magnetically trapped and passing ions, one expects it to have the form of a

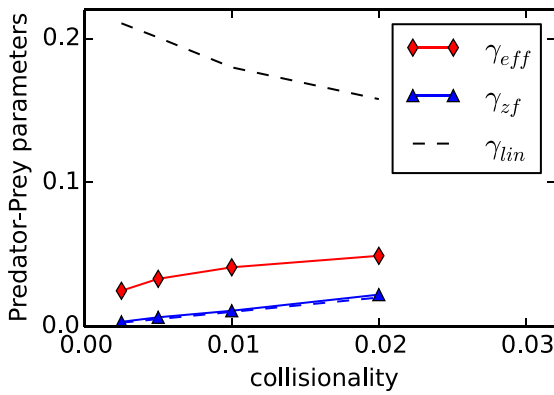


FIG. 2. The effective zonal flow damping rates γ_{zf} , found by fitting gyrokinetic simulations to predator-prey model, which seems to agree rather well with collisional damping (dashed-blue curve), and the effective growth rate γ_{eff} , which is roughly constant in spite of the change of the linear growth rate of the most unstable mode γ_{lin} , demonstrating self-regulation by zonal flow.

drag. As shown in Figs. 2 and 3, the zonal flow damping rates estimated by fitting with the model (blue triangles) coincide with the relevant gyrokinetic collisionalities (blue-dashed curves). In particular, it is shown in Fig. 2 that, when collisionality ν is lowered by a certain factor, the frequency of the predator-prey dynamics is reduced roughly by the same factor. Also, the time honored idea that the fluctuation level goes up with increasing collisionality (because the zonal flow damping increases, and it is the zonal flows that regulate the turbulence level) works rather well.

On the other hand, when density gradient is varied at constant collisionality, the effective damping stays roughly constant [i.e., Fig. 3]. This implies that the Kelvin-Helmholtz (KH)-like instability might play negligible role compared to the collisional damping effect in regulating the predator-prey oscillation for the range of parameters that are considered. In general, it is likely that when the nonlinear damping of the zonal flow becomes important, the simple Lotka-Volterra dynamics gets obscured with other nonlinear effects, so the clean limit cycle behaviour disappears and a direct least squares fitting no longer works.

These results also demonstrate that the effective linear growth rate estimated by fitting to the predator-prey model

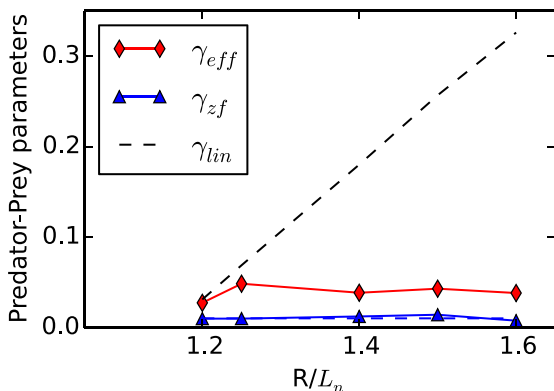


FIG. 3. The effective growth rate γ_{eff} , the effective zonal flow damping rates γ_{zf} , and the linear growth rate of the most unstable mode γ_{lin} as a function of density gradients found by fitting gyrokinetic simulations to predator-prey model.

(red diamonds) stays roughly constant ($\gamma_{eff} \sim 0.02-0.05$), in spite of the variation of the linear growth rate (black dashed curves which vary $\gamma_{lin} \sim 0.05-0.3$) when the R/L_n is increased. This demonstrates self-regulation of the plasma turbulence in the presence of dominant zonal flows. We also note that the level of the effective linear growth roughly agrees with the gyrokinetic “linear” growth rate $\gamma_{gk} \sim 0.05$ modified by the presence of zonal flows at saturation level.¹

It was also observed that the coupling constants (c_1 and c_2) vary strongly with collisionality and density gradient as shown in Figs. 4 and 5. In particular, as density gradients increase, the first coupling constant c_1 rapidly becomes smaller, as shown in Fig. 5. This is consistent with the fact that when the density gradients is increased further (e.g., $R/L_n \sim 1.8$), the simulations show no longer the clear predator-prey dynamics. The results suggest that the weakening of coupling results in the disappearance of the predator-prey dynamics (i.e., more chaotic nonlinear dynamics follow). We note, on the other hand, that as collisionality is lowered γ_{eff} goes down, slowing down the frequency of the oscillation and leading to a Dimits-shift like situation eventually in the collisionless limit. However, as expected, in such a state the average zonal flow level (i.e., the offset of E_v) goes up as well. Moreover, a simple fixed point analysis of the Lotka-Volterra system suggests that (at least for small amplitude of the oscillations) the average zonal flow level should be proportional to $\gamma_{eff}c_1$. This means that the coupling constant c_1 should go down faster than γ_{eff} , as the collisionality decreases, in order that the average zonal flow level goes up. Fig. 6 shows the power spectrum of $|\phi|$ as a function of frequency. As one exits the range of parameters where the predator-prey oscillations can be cleanly identified, multiple frequencies appear (i.e. $\nu = 0.02$). The dominant predator-prey frequency ω_{0max} increases with collisionality ν (top right panel of Fig. 6) as the zonal flows are dumped mostly by collisions.

Finally, we found that the nonlinear damping effects γ_{nl} and $\Delta\omega$ are probably not significant in the present system as long as the clean limit cycle behavior is sustained. As these terms become important, a more complicated model with 3 or more equations is necessary. This particular range of values of the physical parameters for the

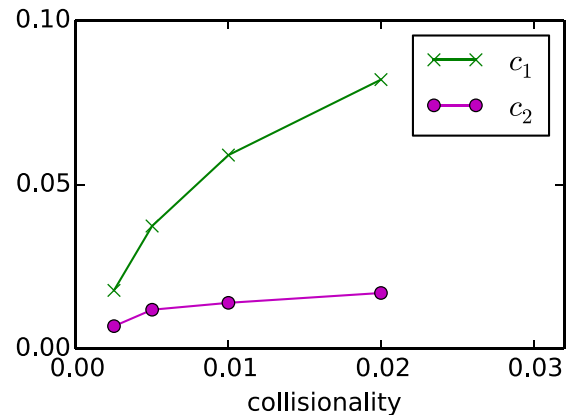


FIG. 4. Coupling parameters as a function of collisionality found by fitting gyrokinetic simulations to the predator-prey model.

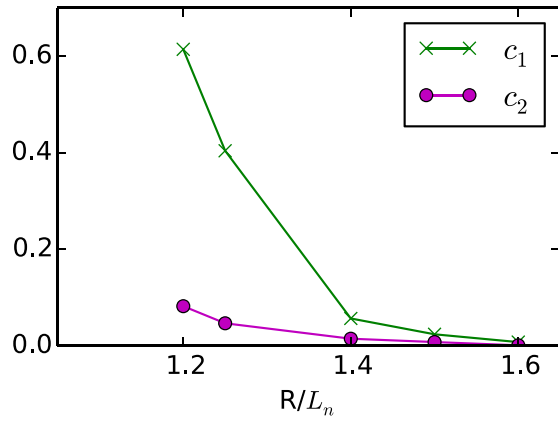


FIG. 5. Coupling parameters found by fitting gyrokinetic simulations to predator-prey model. The couplings become weaker as density gradients increase, consistent with the disappearance of clear predator-prey dynamics of gyrokinetic simulations.

gyrokinetic system is special in that the system with a large degrees of freedom (i.e., the full gyro-kinetic simulation) reduces itself to a system with two, through a process akin to synchronization.^{34–36}

Since the gyrokinetic simulations presented in this letter were performed on a Z-pinch geometry, their direct relevance to magnetized fusion experiments, and in particular, tokamaks are questionable. In particular, the fact that there is no magnetic shear is expected to promote Kelvin-Helmholtz instability of the zonal flow as compared to the tokamak, where the magnetic shear works against the vortex-tube interchange. However, even though magnetic shear is a key aspect of the tokamak confinement, it is mostly a source of complication for understanding the nonlinear predator-prey dynamics. Therefore, simulations in simplified geometry allow a cleaner determination of its constituents where the oscillations can be identified clearly and fitted directly with a simple model.

In tokamaks, limit cycle oscillations akin to predator-prey oscillations were observed during the transition from the low to high confinement regimes (i.e., the so-called I-phase).^{8,9,11} While the experimental oscillations are not as

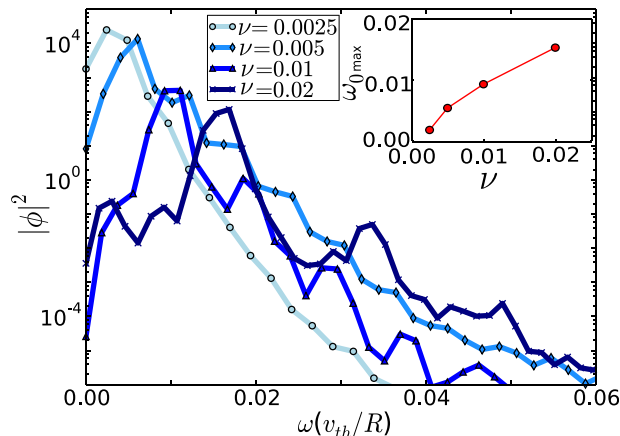


FIG. 6. Power spectrum of $|\phi|^2$ as a function of frequency (main panel), and the dominant predator-prey frequency ω_{0max} for a range of ν (top right panel).

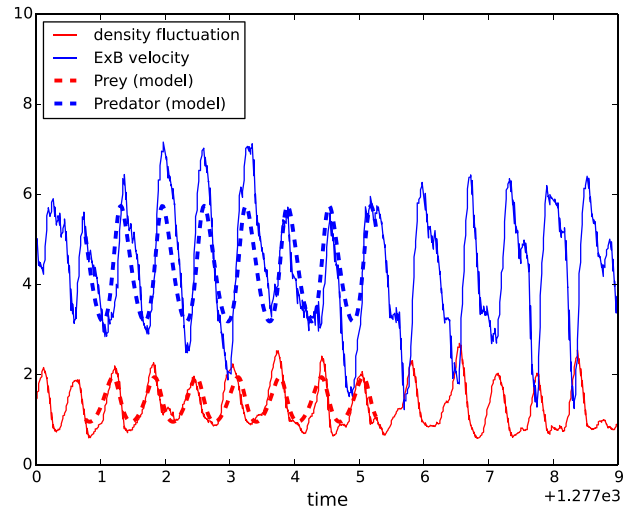


FIG. 7. The data from the DIII-D tokamak, during the I-phase limit cycle oscillations,³⁷ for the $E \times B$ velocity (arbitrary offset) as well as the normalized density fluctuations in arbitrary units, fitted against a basic Lotka-Volterra model.

clean, a direct fit to the experimental data seems possible with the basic algorithm we use here (see Figure 7). The parameters of the fit to the experimental data are found to be approximately $\gamma_{eff} = 0.090$, $\gamma_{zf} = 0.063$, $c_1 = 0.0046$, and $c_2 = 0.031$ in units of c_s/R (assuming $T_e \approx 2$ keV and $R \approx 2.3$ m). The Doppler backscattering (DBS) data that we have used here is from Ref. 37 (the case presented for $R = 2.25$ m) for the $E \times B$ velocity and the normalized density fluctuation levels. Note that the fit is not unique since the data is in arbitrary units, therefore, an offset value has been added to the $E \times B$ velocity and the normalized density fluctuation has been scaled in order to achieve the fit. It is interesting to observe that these parameter values fall within the range for which the gyrokinetics showed predator-prey behaviour.

These results underline the important link between the process of synchronization or entrainment through which a turbulent system reduces its effective degrees of freedom and the I-phase limit cycle oscillations that are observed in the L-H transition in a tokamak. The details of the mechanism of synchronization in different systems may have different origins, the interaction of individual predator-prey oscillators (i.e., 3 fluctuating components of the 4-wave tetrad as the prey and its zonal pair as the predator of a single predator-prey node) may happen through the interaction with the mean $E \times B$ flow as in the experimental case, or through the average phase, in a local gyrokinetic simulation. A flux-driven simulation, which can evolve the profiles, may be closer to the experiment in these aspects, even though it is harder to match the experiment.³⁸ Nonetheless, understanding of coupled drift-wave zonal-flow predator-prey networks requires identification of microscopic interaction mechanisms both in space and in wave-number, which should be developed in future works.

Limit cycle oscillations involving zonal flows and fluctuations that were observed in gyrokinetic simulations in a simplified Z-pinch geometry have been fitted against a

simple predator-prey model of the Lotka-Volterra equations. This allowed a direct extraction of the coefficients of an equivalent predator-prey model. The results show that as long as the clear predator-prey cycle is sustained, the zonal flow damping is collisional, suggesting that when the Kelvin-Helmholtz instability of the zonal flow plays an important role, it breaks-up the clean predator-prey behavior such that fitting with the simple model is no longer possible. This also confirms the basic intuition that increasing the collisionality results in increased transport because of the increased damping of zonal flows, since it is the zonal flows that limit the turbulence decorrelation. Finally within the range of parameters where a clean limit cycle behavior was observed, increasing R/L_n , which results in a clear linear increase of the linear growth rate, does not lead to an increase of the effective growth rate, since the effective growth rate results from a self-organization process between the fluctuations and the zonal flows. This final point may be an annoyance for the quasi-linear modeling of turbulent transport that usually does not take the zonal flows into account. The reduced model such as Ref. 39 takes into account the modification of the zonal flow response, however, ignores the interaction dynamics between zonal flows and turbulence. A fix may be possible by including the self-consistent dynamics with the zonal flows in quasi-linear modeling as is sometimes done in geophysical fluid dynamics (GFD) where zonal flows play an important role as well.⁴⁰ Incidentally this somewhat different approach is called “quasi-linear” in GFD, as it includes the interactions between zonal flows and fluctuations but ignores the fluctuation-fluctuation nonlinearities.

The authors appreciate valuable discussions with T. S. Hahm and Y. Sarazin. This research was supported by the National Science Foundation under Grant No. NSF PHY11-25915 and by the grants from ANR-11-JS56-0008 and IFFERC-Helios.

¹S. Kobayashi and B. N. Rogers, *Phys. Plasmas* **19**, 012315 (2012).

²P. H. Diamond, Y.-M. Liang, B. A. Carreras, and P. W. Terry, *Phys. Rev. Lett.* **72**, 2565 (1994).

³Z. Lin, T. S. Hahm, W. W. Lee, W. M. Tang, and P. H. Diamond, *Phys. Rev. Lett.* **83**, 3645 (1999).

⁴M. A. Malkov, P. H. Diamond, and M. N. Rosenbluth, *Phys. Plasmas* **8**, 5073 (2001).

⁵E. Kim and P. Diamond, *Phys. Plasmas* **10**, 1698 (2003).

⁶G. Tynan, M. Xu, P. Diamond, J. Boedo, I. Cziegler, N. Fedorczak, P. Manz, K. Miki, S. Thakur, L. Schmitz *et al.*, *Nucl. Fusion* **53**, 073053 (2013).

⁷K. Miki, P. H. Diamond, Ö. D. Gürcan, G. R. Tynan, T. Estrada, L. Schmitz, and G. S. Xu, *Phys. Plasmas* **19**, 092306 (2012).

⁸T. Estrada, T. Happel, C. Hidalgo, E. Ascasibar, and E. Blanco, *Europhys. Lett.* **92**, 35001 (2010).

⁹G. D. Conway, C. Angioni, and F. Ryter *et al.*, *Phys. Rev. Lett.* **106**, 065001 (2011).

¹⁰P. Manz, G. S. Xu, B. N. Wan, H. Q. Wang, H. Y. Guo, I. Cziegler, N. Fedorczak, C. Holland, S. H. Müller, S. C. Thakur *et al.*, *Phys. Plasmas* **19**, 072311 (2012).

¹¹L. Schmitz, L. Zeng, T. L. Rhodes, J. C. Hillesheim, E. J. Doyle, R. J. Groebner, W. A. Peebles, K. H. Burrell, and G. Wang, *Phys. Rev. Lett.* **108**, 155002 (2012).

¹²J. Cheng, J. Dong, K. Itoh, L. Yan, W. Hong, K. Zhao, Z. Huang, X. Ji, W. Zhong, D. Yu *et al.*, *Nucl. Fusion* **54**, 114004 (2014).

¹³A. I. Smolyakov, P. H. Diamond, and V. I. Shevchenko, *Phys. Plasmas* **7**, 1349 (2000).

¹⁴Ö. D. Gürcan, X. Garbet, P. Hennequin, P. H. Diamond, A. Casati, and G. L. Falchetto, *Phys. Rev. Lett.* **102**, 255002 (2009).

¹⁵V. Berionni and Ö. D. Gürcan, *Phys. Plasmas* **18**, 112301 (2011).

¹⁶P. Morel, Ö. D. Gürcan, and V. Berionni, *Plasma Phys. Controlled Fusion* **56**, 015002 (2014).

¹⁷W. Dorland, F. Jenko, M. Kotschenreuther, and B. N. Rogers, *Phys. Rev. Lett.* **85**, 5579 (2000).

¹⁸M. Kotschenreuther, G. Rewoldt, and W. M. Tang, *Comput. Phys. Commun.* **88**, 128 (1995).

¹⁹P. H. Diamond, S.-I. Itoh, K. Itoh, and T. S. Hahm, *Plasma Phys. Controlled Fusion* **47**, R35 (2005).

²⁰N. S. Goel, S. C. Maitra, and E. W. Montroll, *Rev. Mod. Phys.* **43**, 231 (1971).

²¹R. D. Holt and J. Pickering, *Am. Nat.* **126**, 196 (1985).

²²A. d’Onofrio, *Physica D* **208**, 131 (2005).

²³L. C. Miranda and C. A. Lima, *Technol. Forecasting Soc. Change* **80**, 1179 (2013).

²⁴J. González-Avellaa, M. Cosenzac, and M. S. Miguel, *Physica A* **399**, 24 (2014).

²⁵A. C. Boxer, R. Bergmann, J. L. Ellsworth, D. T. Garnier, J. Kesner, M. E. Mauel, and P. Woskov, *Nat. Phys.* **6**, 207 (2010).

²⁶H. Saitoh, Y. Yano, Z. Yoshida, M. Nishiura, J. Morikawa, Y. Kawazura, T. Nogami, and M. Yamasaki, *Phys. Plasmas* **22**, 024503 (2015).

²⁷P. Ricci, B. N. Rogers, and W. Dorland, *Phys. Rev. Lett.* **97**, 245001 (2006).

²⁸S. Kobayashi, B. N. Rogers, and W. Dorland, *Phys. Rev. Lett.* **103**, 055003 (2009).

²⁹S. Kobayashi, B. N. Rogers, and W. Dorland, *Phys. Rev. Lett.* **105**, 235004 (2010).

³⁰P. Ricci, B. N. Rogers, W. Dorland, and M. Barnes, *Phys. Plasmas* **13**, 062102 (2006).

³¹H. D. I. Abarbanel, R. Brown, J. J. Sidorowich, and L. S. Tsimring, *Rev. Mod. Phys.* **65**, 1331 (1993).

³²E. Baake, M. Baake, H. G. Bock, and K. M. Briggs, *Phys. Rev. A* **45**, 5524 (1992).

³³D. Brewer, M. Barenco, R. Callard, M. Hubank, and J. Stark, *Philos. Trans. R. Soc. London, Ser. A* **366**, 519 (2008).

³⁴L. M. Pecora and T. L. Carroll, *Phys. Rev. Lett.* **64**, 821 (1990).

³⁵M. G. Rosenblum, A. S. Pikovsky, and J. Kurths, *Phys. Rev. Lett.* **76**, 1804 (1996).

³⁶B. Blasius, A. Huppert, and L. Stone, *Nature* **399**, 354 (1999).

³⁷L. Schmitz, L. Zeng, T. Rhodes, J. Hillesheim, W. Peebles, R. Groebner, K. Burrell, G. McKee, Z. Yan, G. Tynan *et al.*, *Nucl. Fusion* **54**, 073012 (2014).

³⁸Y. Sarazin, V. Grandgirard, J. Abiteboul, S. Allfrey, X. Garbet, P. Ghendrih, G. Latu, A. Strugarek, and G. Dif-Pradalier, *Nucl. Fusion* **50**, 054004 (2010).

³⁹M. Nunami, T.-H. Watanabe, and H. Sugama, *Phys. Plasmas* **20**, 092307 (2013).

⁴⁰K. Srinivasan and W. R. Young, *J. Atmos. Sci.* **69**, 1633 (2012).